Immunity
Article

Tumor Necrosis Factor Receptor-Associated Factor 3 Is a Critical Regulator of B Cell Homeostasis in Secondary Lymphoid Organs

Ping Xie,[1] Laura L. Stunz,[1] Karen D. Larison,[1] Baoli Yang,[3] and Gail A. Bishop[1,2,4,*]
[1]Department of Microbiology
[2]Department of Internal Medicine
[3]Department of Obstetrics and Gynecology
The University of Iowa, Iowa City, IA 52242, USA
[4]Veterans Affairs Medical Center, Iowa City, IA 52242, USA
*Correspondence: gail-bishop@uiowa.edu
DOI 10.1016/j.immuni.2007.07.012

SUMMARY

Tumor necrosis factor receptor-associated factor 3 (TRAF3) is an adaptor protein that directly binds to a number of receptors of the tumor necrosis factor receptor (TNF-R) superfamily. Despite in vitro evidence that TRAF3 plays diverse roles in different cell types, little is known about the in vivo functions of TRAF3. To address this gap in knowledge and to circumvent the early lethal effect of TRAF3 null mutations, we generated conditional TRAF3-deficient mice. B-cell-specific *Traf3*$^{-/-}$ mice displayed severe peripheral B cell hyperplasia, which culminated in hyperimmunoglobulinemia and increased T-independent antibody responses, splenomegaly and lymphadenopathy. Resting splenic B cells from these mice exhibited remarkably prolonged survival ex vivo independent of B cell activating factor and showed increased amounts of active nuclear factor-κB2 but decreased amounts of nuclear protein kinase Cδ. Furthermore, these mice developed autoimmune manifestations as they aged. These findings indicate that TRAF3 is a critical regulator of peripheral B cell homeostasis and may be implicated in the regulation of peripheral self-tolerance induction.

INTRODUCTION

Tumor necrosis factor receptor-associated factor 3 (TRAF3), a member of the TRAF family of cytoplasmic adaptor proteins, is exploited for signaling by a number of receptors of the tumor necrosis factor receptor (TNF-R) superfamily as well as the Epstein-Barr virus (EBV)-encoded oncoprotein latent membrane protein 1 (LMP1) (Bishop, 2004; Miller et al., 2006; Wajant et al., 2001). TRAF3 directly binds to almost all TNF-R-superfamily receptors that do not contain death domains, including CD40, receptors for B cell activating factor (BAFF) and a proliferation-inducing ligand (APRIL), lymphotoxin β receptor (LTβR), CD27, CD30, receptor activator of NF-κB (RANK), herpesvirus entry mediator (HVEM), ectodysplasin A receptor (EDAR), X-linked ectodermal dysplasia receptor (XEDAR), 4-1BB, OX-40, and glucocorticoid-induced TNF-R-related gene (GITR). Among these, BAFF receptors and CD40 are pivotal in the physiology of B lymphocytes, the only mammalian cell type that can produce antibodies.

BAFF is a crucial B cell survival factor, binding to the following three receptors of the TNF-R superfamily: BCMA, TACI, and BAFF-R (Mackay et al., 2003; Miller et al., 2006). TACI and BCMA are also bound by APRIL, a TNF family member closely related to BAFF. Interestingly, BAFF-R appears to be the sole mediator of BAFF-mediated B cell-survival signals. Only BAFF-R-deficient mice recapitulate the phenotype of BAFF-deficient mice, which display almost complete loss of mature B lymphocytes and marginal zone B cells and deficiency in mounting T-dependent humoral responses (Schiemann et al., 2001; Shulga-Morskaya et al., 2004). In contrast, B cell maturation in BCMA-deficient, TACI-deficient, and BCMA and TACI double-deficient mice is normal or enhanced (Mackay et al., 2003; Shulga-Morskaya et al., 2004). The two predominant signaling pathways initiated by BAFF and BAFF-R interactions shown to promote B cell survival are the alternative NF-κB (NF-κB2) pathway and inhibition of protein kinase Cδ (PKCδ) nuclear translocation (Claudio et al., 2002; Mecklenbrauker et al., 2004). To date, the only TRAF protein shown to directly interact with BAFF-R is TRAF3 (Miller et al., 2006). A recent study reported that mutation of the putative TRAF-binding motif of BAFF-R abolishes its interaction with TRAF3 and its ability to induce NF-κB2 activation in the mouse B cell line M12, suggesting that TRAF3 is critical for BAFF-R-mediated NF-κB2 activation in B cells (Morrison et al., 2005).

CD40 and its ligand CD154 are obligatory for T cell-dependent B cell activation, regulating formation of germinal centers, immunoglobulin (Ig) isotype switching, and

development of memory B cells (Bishop, 2004; Quezada et al., 2004). All these processes are severely impaired in CD40-deficient or CD154-deficient mice or in human patients carrying *CD40LG* mutations (Grammer and Lipsky, 2000). Upon ligand binding, CD40 recruits TRAF1, TRAF2, TRAF3, TRAF5, and TRAF6 directly or indirectly to its signaling complex (Bishop, 2004; Grammer and Lipsky, 2000; Xie et al., 2006). TRAF recruitment in turn triggers multiple signaling cascades, including activation of kinases (such as p38, JNK, ERK, and Akt) and transcription factors (such as NF-κB and AP-1). This ultimately leads to proliferation, upregulation of adhesion and costimulatory molecules, and secretion of antibodies and cytokines (Bishop, 2004; Grammer and Lipsky, 2000). By using *Traf3*$^{-/-}$ B cell lines, we previously showed that CD40-induced JNK activation and antibody secretion are enhanced in the absence of TRAF3 (Xie et al., 2004). Conversely, signaling by LMP1, the viral oncogenic mimic of CD40, is defective in *Traf3*$^{-/-}$ B cells (Xie and Bishop, 2004; Xie et al., 2004). LMP1-induced activation of JNK, p38, and NF-κB and upregulation of CD23 and CD80, as well as antibody secretion, are profoundly impaired by TRAF3 deficiency (Xie and Bishop, 2004; Xie et al., 2004). Thus, CD40 and LMP1 use TRAF3 in sharply different ways in B cells.

In addition to directly interacting with the TNF-R superfamily receptors, TRAF3 has recently been found to be involved in production of type I interferon and IL-10 induced by Toll-like receptors (TLRs) in macrophages and dendritic cells through association with TRIF, an adaptor protein for TLRs (Hacker et al., 2006; Oganesyan et al., 2006). Taken together, these in vitro observations indicate that TRAF3 can play important and diverse roles depending on the specific interacting receptor and cellular context. This warrants further in vivo investigation so that the physiological functions of TRAF3 in the intact animal can be understood.

Mice genetically deficient in the gene encoding TRAF3 die within 10 days after birth, demonstrating the ubiquitous and critical developmental functions of TRAF3 (Xu et al., 1996). However, assessment of specific functions of TRAF3 in the immune system and in signaling by the TNF-R superfamily or TLRs in tissues of adult mice is compromised by the early lethality of *Traf3*$^{-/-}$ mice. To circumvent this problem, we employed a conditional gene targeting strategy through Cre-loxP-mediated recombination and generated conditional TRAF3-deficient mice, which allow the deletion of the *Traf3* gene in specific cell types or tissues. We found that specific ablation of the gene encoding TRAF3 in the B cell lineage led to remarkably prolonged B cell survival and greatly expanded B cell compartments in secondary lymphoid organs with markedly increased numbers of T2 transitional, marginal zone and follicular B cells. This culminated in splenomegaly and lymphadenopathy, hyperimmunoglobulinemia, and autoimmune reactivity. Our findings reveal a critical role for TRAF3 in regulating peripheral B cell homeostasis and implicate TRAF3 in peripheral self-tolerance induction.

RESULTS

Conditional Deletion of the *Traf3* Gene

By using a conditional gene targeting approach, we generated mouse embryonic stem cells and a new mouse strain in which the *Traf3* gene is modified with insertions of two loxP sequences, recognition sites of the DNA recombinase Cre, into the introns flanking the first two coding exons of *Traf3* (Figures S1 and S2 in the Supplemental Data available online). Such "flox" modification of the *Traf3* gene (*Traf3*^{flox}) does not affect the expression of *Traf3* unless Cre-mediated deletion of the first two coding exons occurs, and such a deletion leads to a *Traf3* null allele (*Traf3*$^{\Delta}$) (Figure S1A). Mice homozygous for the floxed *Traf3* allele (*Traf3*$^{flox/flox}$) were fertile and healthy.

To delete the loxP-flanked *Traf3* alleles specifically in B lymphocytes, we used a transgenic mouse strain expressing Cre under the control of the endogenous *Cd19* locus, which provides a B cell-specific source of Cre (Rickert et al., 1997). It has been previously shown that *Cd19*^{Cre} mediates deletion of loxP-flanked gene segments specifically in the B cell lineage and that the deletion efficiency is 75%–80% in the bone marrow (BM) and >95% in splenic B cells (Pasparakis et al., 2002; Rickert et al., 1997). *Traf3*$^{flox/flox}$*Cd19*$^{+/Cre}$ mice were born at the expected Mendelian frequencies and survive and breed normally. We verified excision of the first two coding exons of the *Traf3* gene and the elimination of TRAF3 protein expression in splenic B cells of *Traf3*$^{flox/flox}$*Cd19*$^{+/Cre}$ mice (B-*Traf3*$^{-/-}$ mice) by genomic PCR and western-blot analysis, respectively (Figure S1C and Figure 1A).

Splenomegaly and Lymphoadenopathy with Expanded B Cell Compartments in B-*Traf3*$^{-/-}$ Mice

Adult B-*Traf3*$^{-/-}$ mice exhibited greatly enlarged spleens and lymph nodes (LNs) compared to those from *Traf3*$^{flox/flox}$ littermate control (LMC) or wild-type mice (Figure 1B, Figure S1A, and data not shown). In contrast, the thymus size of B-*Traf3*$^{-/-}$ mice was comparable to that of LMC mice, and the spleen size of *Traf3*$^{+/flox}$*Cd19*$^{+/Cre}$ mice was similar to that of LMC mice (data not shown). Histochemical staining of LN sections revealed that B-*Traf3*$^{-/-}$ mice had increased size and numbers of lymphoid follicles (Figure S3B).

To determine which cell types were expanded in the enlarged spleen and LNs of B- *Traf3*$^{-/-}$ mice, we performed cellularity analysis by immunofluorescence staining and flow cytometry. Proportions and absolute numbers of B cells (B220^{+} or IgM^{+}) in both spleen and LNs were markedly increased, whereas the proportion of T cells (CD3^{+}) was reduced in B-*Traf3*$^{-/-}$ mice (Figure 1C, Figure S3C, and Table S1). Further detailed analysis of B cell subsets revealed that the numbers of T2 transitional (B220^{+}AA4.1^{+}IgM^{+}CD23^{+} or B220^{+}AA4.1^{+}IgM^{+}IgD^{+}), follicular (B220^{+}IgM^{+}CD21^{int}CD23^{hi}), and marginal zone (B220^{+}IgM^{+}CD21^{hi}CD23^{int} or B220^{+}IgM^{+}CD1d^{+}CD9^{+}) B cells were vastly increased in the spleen of B-*Traf3*$^{-/-}$ mice (Figures 1D and 1E and Table S1). Particularly,

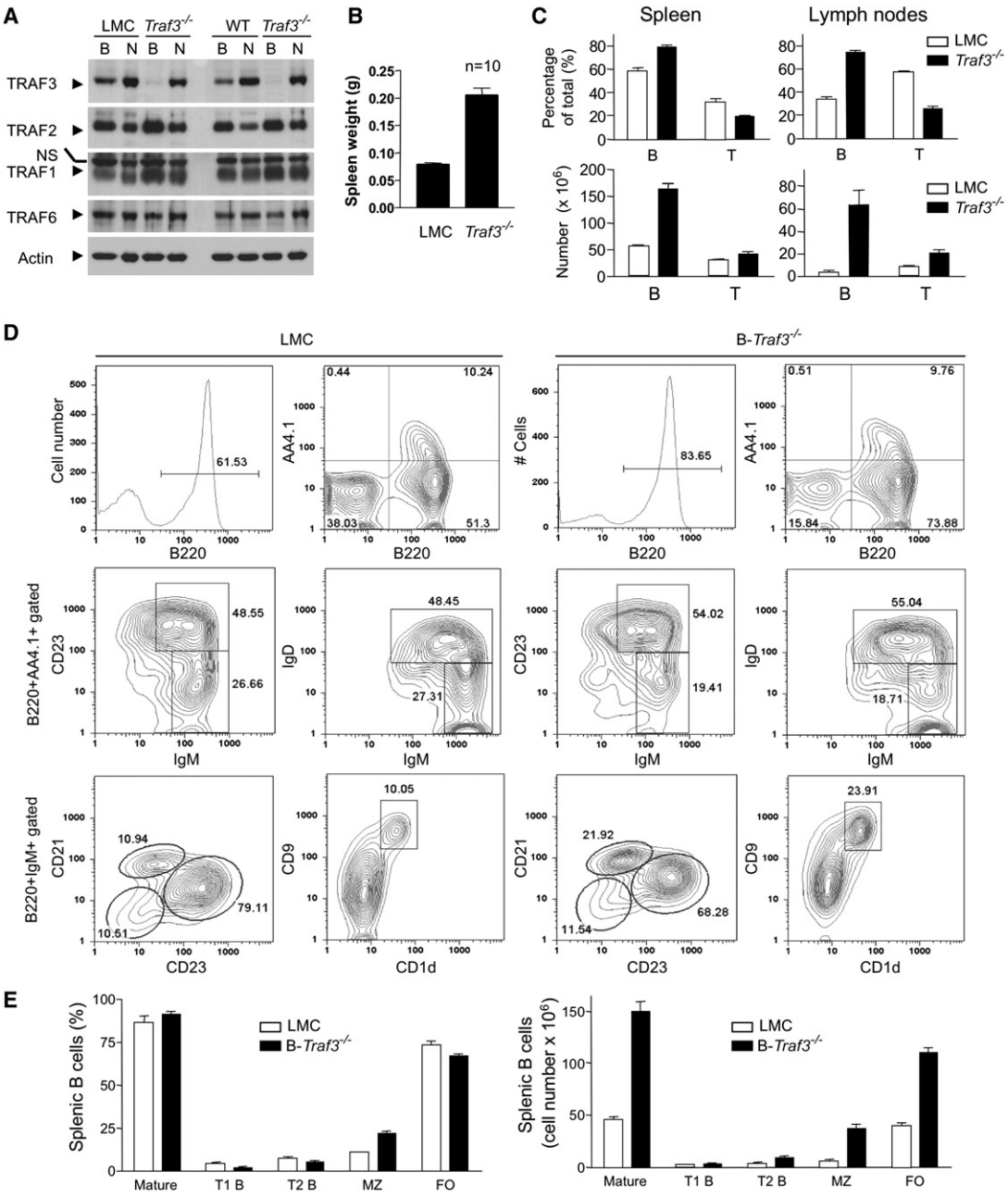

Figure 1. Expanded B Cell Compartments in Spleens and Lymph Nodes of B-*Traf3*$^{-/-}$ Mice

(A) Verification of *Traf3* deletion in B cells by immunoblot analysis. Splenic B cells were purified from LMC and B-*Traf3*$^{-/-}$ (*Traf3*$^{-/-}$) mice by negative selection with CD43-magnetic beads. Total cellular proteins were extracted from both the purified B cells (B) and the CD43^{+} (mainly non-B) cells (N). The same protein blot was first immunoblotted for TRAF3, and then it was stripped and reprobed for TRAF2, TRAF1, TRAF6, and actin. NS, non-specific band. Results shown are representative of three independent experiments.

(B) Enlarged spleen of B-*Traf3*$^{-/-}$ mice. The graph depicts spleen weights (mean ± SEM, n = 10 for each group of mice).

(C) Percentages and numbers of B and T cells in spleens and LNs of LMC and B-*Traf3*$^{-/-}$ mice. B cells and T cells were identified by FACS analysis with markers described in Table S1. The graph depicts the results of four independent experiments (mean ± SEM).

(D) Representative FACS histograms or contour plots of splenic B cells of LMC and B-*Traf3*$^{-/-}$ mice. FACS profiles were scatter-gated on single lymphocytes. T1, T2, follicular (FO), and marginal zone (MZ) B cell populations were identified with markers described in Table S1. Similar results were observed in three additional experiments.

(E) Percentages (among total B cells) and numbers of splenic B cell subsets of LMC and B-*Traf3*$^{-/-}$ mice. The graph depicts the results of four independent experiments (mean ± SEM). Mice analyzed were 8 to 12 weeks old.

both the percentage and number of marginal zone B cells were increased in B-*Traf3*$^{-/-}$ mice, and such an expansion of marginal zone B cells was also verified by immunofluorescence staining of spleen cryosections (Figure S6). Interestingly, the expression of CD21 and CD23, two markers for peripheral B cell maturation, were increased in both splenic and LN B cells of B-*Traf3*$^{-/-}$ mice (Figure S4). However, proportions of B-1a (B220^{+}CD11b^{+}CD5^{+}), B-1b (B220^{+}CD11b^{+}CD5^{-}), and B-2 (B220^{+}CD11b^{-}CD23^{+}) subsets in peritoneal lavages from B-*Traf3*$^{-/-}$ mice were normal compared to those from LMC mice (data not shown). In addition, thymic T cell subsets of B-*Traf3*$^{-/-}$ mice were unchanged relative to those of LMC mice (Figure S5). In summary, these results indicate that the splenomegaly and lymphadenopathy of B-*Traf3*$^{-/-}$ mice were due to massive expansion of B cell compartments, and *Traf3*$^{-/-}$ B cell expansion was evident from the T2 transitional B cell stage onward. Because TRAF3 ablation specifically occurred in the B cell lineage but not in non-B cells, we conclude that the B cell hyperplasia observed in B-*Traf3*$^{-/-}$ mice is B cell autonomous.

Spontaneous Germinal Center B Cells in B-*Traf3*$^{-/-}$ Mice

We examined splenic microarchitecture of B-*Traf3*$^{-/-}$ mice by immunohistochemical staining and microscopy. Consistent with flow cytometric data, B-*Traf3*$^{-/-}$ mice had enlarged white pulp with expanded B cell follicles compared to LMC mice (Figure 2A). However, the overall organization of B cell follicles (IgM^{+}, blue), T cell zones (CD3^{+}, red), and germinal center (GC) (PNA^{+}, green) were otherwise normal in B-*Traf3*$^{-/-}$ mice immunized with sheep red blood cells (SRBCs) (Figure 2A). Notably, 60% (n = 10) of unimmunized B-*Traf3*$^{-/-}$ mice manifested numerous spontaneous GCs in the spleen, and these spontaneous GCs were not observed in unimmunized LMC mice (Figures 2A–2C). Flow-cytometric analysis revealed that *Traf3*$^{-/-}$ splenic GC B (B220^{+}PNA^{+}) cells expressed increased surface IgM and IgG compared to LMC B cells (Figure 2D) and that GC B cells are CD38^{low} and CD95^{high} relative to non-GC B (B220^{+}PNA^{-}) cells in both LMC and B-*Traf3*$^{-/-}$ mice (Figure S14). Taken together, these results suggest that some *Traf3*$^{-/-}$ B cells may be activated by endogenous antigens in mice.

Hyperimmunoglobulinemia and Enhanced T Independent Antibody Responses in B-*Traf3*$^{-/-}$ Mice

The primary function of B cells is to produce immunoglobulins. Basal serum Ig isotypes IgM, IgG2a, IgG2b, IgG3, and IgA were elevated 2- to 5-fold in B-*Traf3*$^{-/-}$ mice compared to those observed in LMC mice as measured by enzyme-linked immunosorbent analysis (ELISA) (Figure 3A). In contrast, basal serum titers of IgG1 and IgE were unaltered (Figure 3A). In response to the challenge of a T independent antigen (T-I Ag), trinitrophenyl (TNP)-Ficoll, B-*Traf3*$^{-/-}$ mice developed higher titers of TNP-specific IgM, IgG1, IgG2a, IgG2b, and IgG3 antibodies as compared to LMC mice (Figure 3B). Interestingly, after immunization with a T dependent (T-D) Ag, TNP-KLH, B-*Traf3*$^{-/-}$ mice showed an increased TNP-specific IgM response but a normal TNP-specific IgG1 response as compared to the response shown by LMC mice (Figure 3C). Taken together, these results reveal that T-I antibody responses were increased, but the T-D IgG1 response was unaltered in B-*Traf3*$^{-/-}$ mice.

Prolonged Survival of *Traf3*$^{-/-}$ Resting Splenic B Cells Ex Vivo

Expansion of B cell compartments in secondary lymphoid organs may result from increased output from BM, enhanced proliferation, or prolonged lifespan of peripheral B cells. To evaluate which of these contributed to the B cell hyperplasia in B-*Traf3*$^{-/-}$ mice, we first analyzed proportions and numbers of B cell precursors in BM. Proportions and numbers of pro-B (B220^{+}IgM^{-}c-Kit^{+}CD25^{-}), pre-B (B220^{+}IgM^{-}c-Kit^{-}CD25^{+}), immature (B220^{+}AA4.1^{+}IgM^{+}IgD^{-}), and recirculating mature (B220^{+}AA4.1^{-}IgM^{+}IgD^{+}) B cells in BM of B-*Traf3*$^{-/-}$ mice remained similar to those observed in LMC mice (Figure S7 and Table S1). These data, together with the evidence that the numbers of T1 transitional B cells were only slightly increased (approximately 1.4 fold) in B-*Traf3*$^{-/-}$ mice (Figure 1E and Table S1), suggest that the increase, if any, in production of immature B cells in the BM of B-*Traf3*$^{-/-}$ mice is likely to be quite modest.

We next sought to investigate the survival and proliferation capacity of freshly isolated *Traf3*$^{-/-}$ resting splenic B cells ex vivo. When cultured ex vivo with no treatment, *Traf3*$^{-/-}$ resting splenic B cells exhibited greatly expanded survival capacity compared to LMC B cells (Figure 4A). Approximately 30% of *Traf3*$^{-/-}$ B cells remained alive even on day 16 of culture, and BAFF treatment did not further improve their survival (Figure 4A and data not shown). Analysis of cell-cycle distribution by propidium iodide staining and flow cytometry showed that in sharp contrast to LMC B cells, *Traf3*$^{-/-}$ B cells did not undergo spontaneous apoptosis ex vivo even by day 6 of culture (Figure 4B). Results from both cell-cycle analysis and CFSE-dilution experiments demonstrated an unaltered proliferation response in *Traf3*$^{-/-}$ B cells after stimulation with CD40 or CD40 in combination with BCR or IL-4 (Figure S8 and Figure 4C). The enhanced CD40-induced proliferation response in *Traf3*$^{-/-}$ B cells (Figure 4A) is likely to be secondary to their prolonged survival (Figure 4B). Thus, our data indicate that TRAF3 deficiency does not induce proliferation, but it can protect splenic B cells from apoptosis and lead to prolonged survival capacity independent of BAFF.

Lack of Involvement of Soluble Factors in Enhanced Lifespan of *Traf3*$^{-/-}$ B Cells

The prolonged survival of *Traf3*$^{-/-}$ B cells could not be attributed to higher expression of BAFF receptors or CD40 because the expression of BAFF-R, TACI, BCMA, and CD40 in *Traf3*$^{-/-}$ resting splenic B cells, either freshly isolated or after stimulation with BAFF or anti-CD40, were

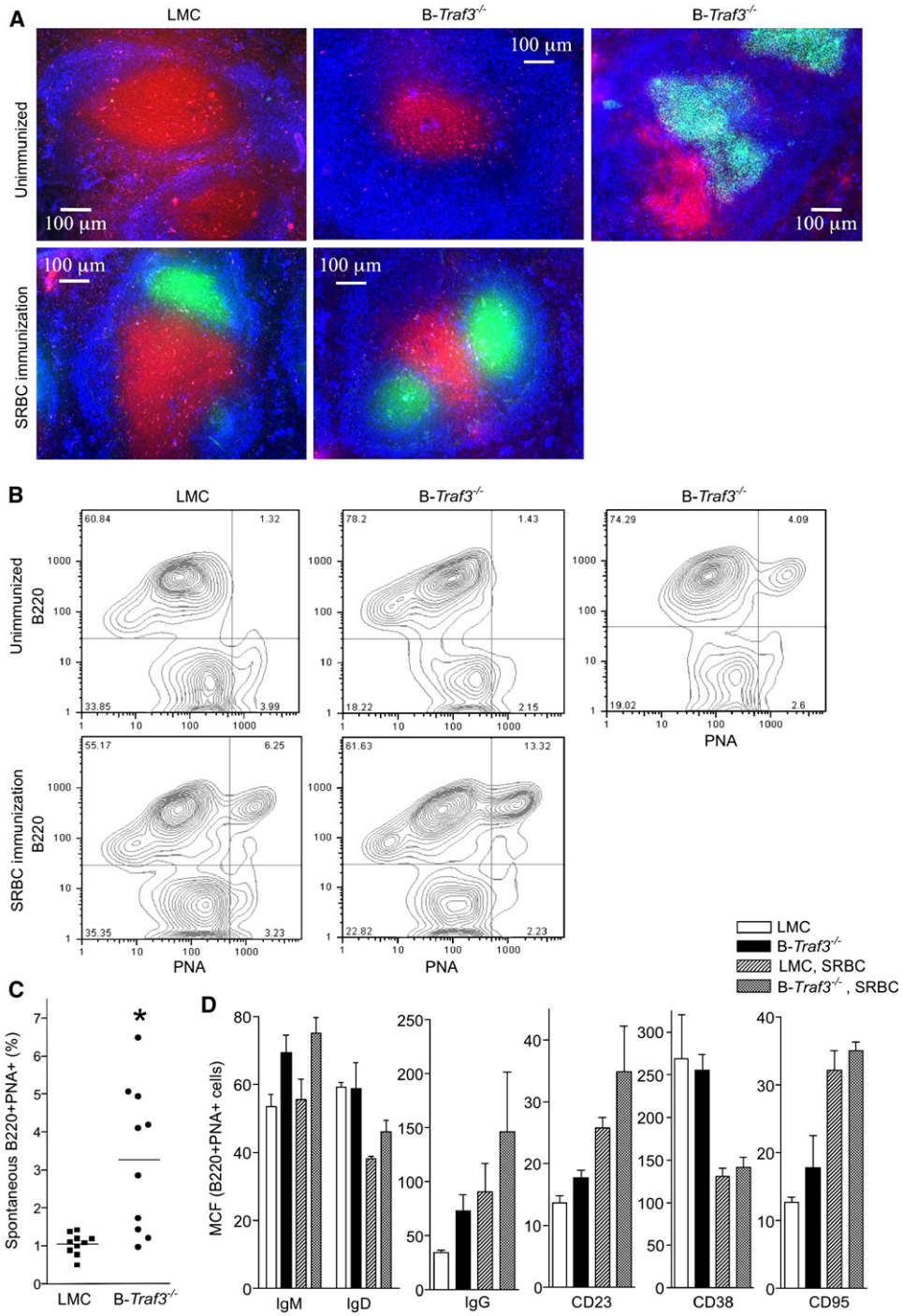

Figure 2. Spontaneous Germinal Centers in B-*Traf3*$^{-/-}$ Mice

(A) Splenic architecture of LMC and B-*Traf3*$^{-/-}$ mice. Frozen sections were prepared from spleens of naive mice or mice immunized with SRBC at 11 days postimmunization, and sections were stained with PNA-FITC (green), anti-IgM-Alexa Fluor 350 (blue), and anti-CD3-PE (red).

(B) GC B cells analyzed by FACS analysis. Representative FACS contour plots of splenocytes of LMC and B-*Traf3*$^{-/-}$ mice are shown. Similar results were observed in two additional experiments.

(C) Percentage of spontaneous GC B cells (B220+PNA^{+}) of LMC and B-*Traf3*$^{-/-}$ mice (n = 10 for each group of mice). *, very significantly different from LMC mice (t test, $p < 0.005$).

(D) Distinct expression profile of GC B cells of B-*Traf3*$^{-/-}$ mice. Splenocytes of naive mice or mice immunized with SRBC at 11 days postimmunization were analyzed by FACS staining. The graph depicts the mean channel fluorescence (MCF) of IgM, IgD, IgG, CD23, CD38, and CD95 expression on B220^{+}PNA^{+}-gated splenocytes. Data shown are the results of three independent experiments (mean ± SEM). Mice analyzed were 10 to 12 weeks old.

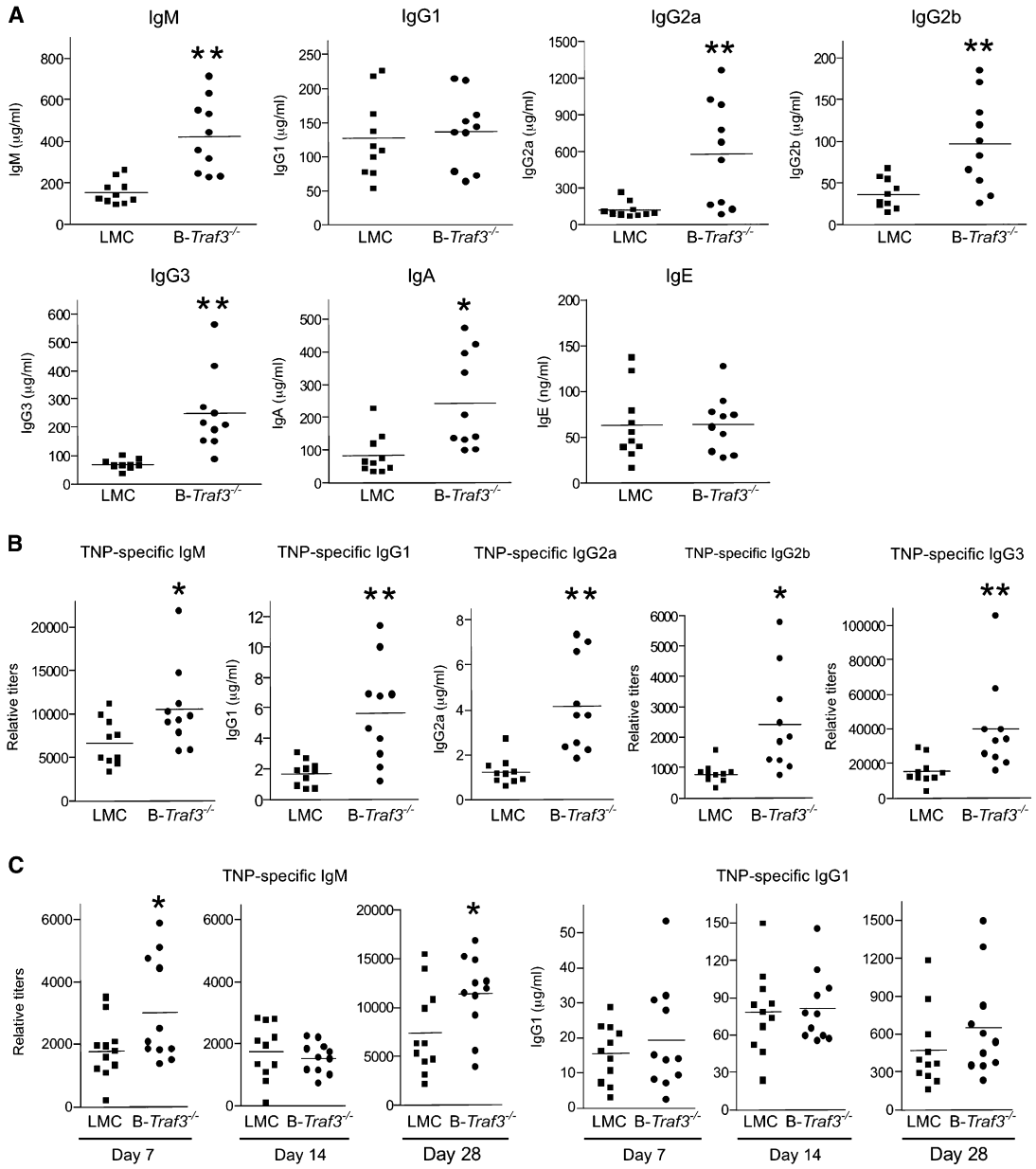

Figure 3. Altered Antibody Responses in B-*Traf3*$^{-/-}$ Mice

(A) Basal serum titers of Ig isotypes. Sera from naive LMC and B-*Traf3*$^{-/-}$ mice (n = 10 for each group) were tested for IgM, IgG1, IgG2a, IgG2b, IgG3, and IgE by ELISA. Mice analyzed were 10 to 12 weeks old. (B) T-I antibody responses. Mice (8-10 weeks old, n = 10 for each group) were immunized with the T-I Ag TNP-Ficoll in Alum, and sera were collected on day 10 after immunization. Serum titers of anti-TNP IgM, IgG1, IgG2a, IgG2b and IgG3 were analyzed by ELISA. (C) T-D antibody responses. Mice (8-10 weeks old, n = 11 for each group) were immunized with the T-D Ag TNP-KLH in Alum, and boosted on day 21 after the first immunization. Sera were collected on day 7, 14 and 28 after the first immunization. Serum titers of anti-TNP IgM and IgG1 were measured by ELISA. Multiple serial dilutions of each serum sample were tested to ensure the readout is within the linear range of the assay. Relative titer = A405 value x 10 x Dilution factor. TNP-specific Ig titers in pre-immune sera (with 1:100 dilution) of both littermate control and B-*Traf3*$^{-/-}$ mice were below the detection limit of ELISA. *, significantly different from LMC (t test, $p < 0.05$); **, very significantly different from LMC (t test, $p < 0.01$).

identical to those detected in LMC B cells (Figure S9 and data not shown). We also evaluated the possibility that death-receptor-mediated apoptotic pathways may be generally impaired in the absence of TRAF3. However, Fas-mediated apoptosis in *Traf3*$^{-/-}$ B cells was intact, and induction of Fas expression by CD40 stimulation was unaffected by TRAF3 deficiency (Figure S10), indicating that extrinsic apoptotic pathways are not detectably impaired in *Traf3*$^{-/-}$ B cells. In addition, results of transwell coculture experiments showed that coculture of

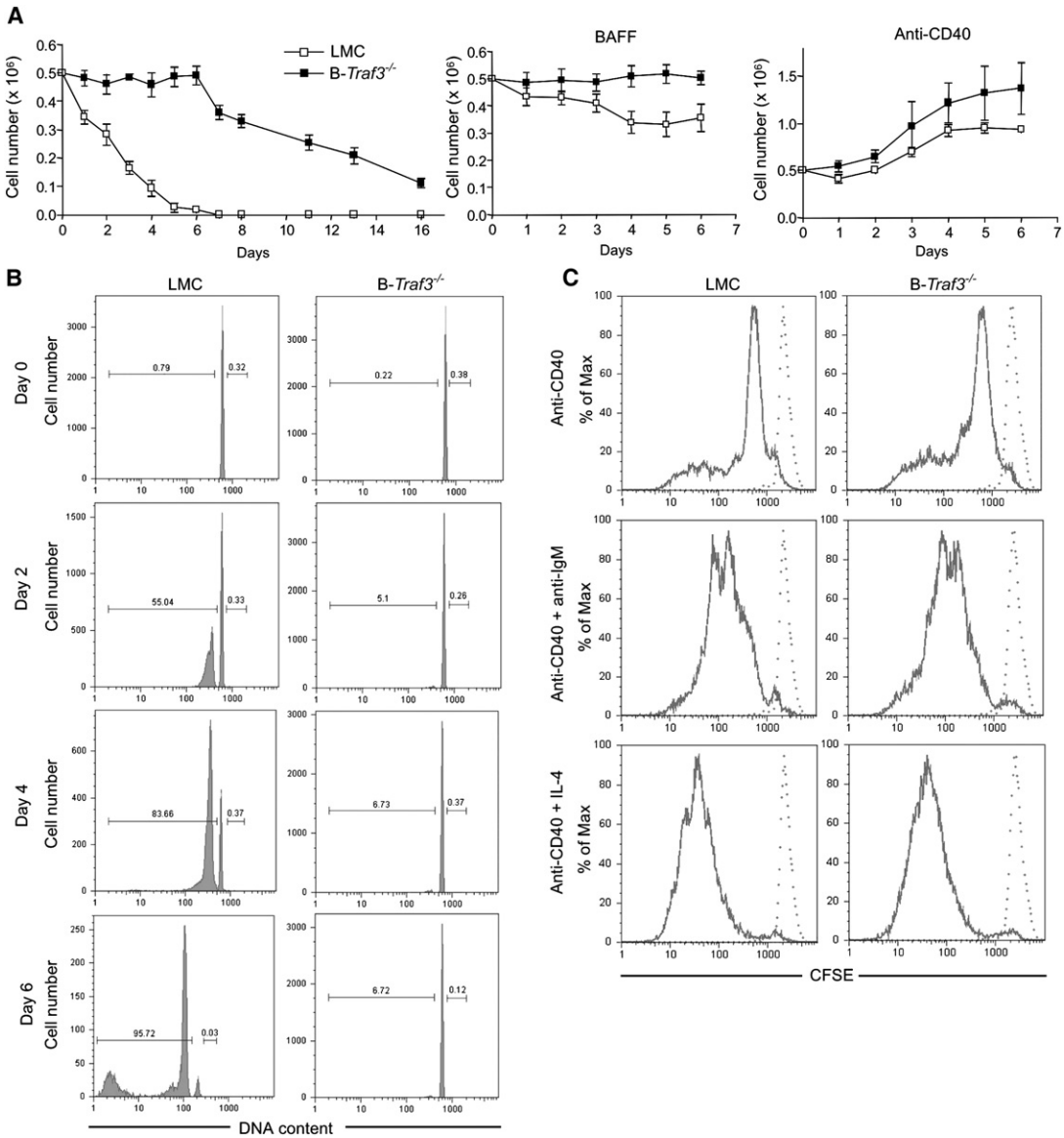

Figure 4. Prolonged survival of *Traf3*$^{-/-}$ resting splenic B cells ex vivo

Resting splenic B cells were purified from 8- to 12- week-old LMC and B-*Traf3*$^{-/-}$ mice and were cultured in the absence or presence of stimulation as indicated.

(A) B cell survival ex vivo. The numbers of viable cells at each time point were determined by staining with Trypan blue. Data shown are results of three independent experiments (mean ± SEM).

(B) Cell-cycle analysis by PI staining and FACS. Representative histograms of PI staining are shown, and percentage of apoptotic cells (DNA content < 2n) and proliferating cells (2n < DNA content ≤ 4n) are indicated.

(C) B cell proliferation analyzed by CFSE labeling. Dashed FACS profile shows CFSE signals of freshly labeled cells, whereas solid profile shows diluted CFSE signals of cells cultured ex vivo for 4 days in the presence of indicated stimulation. Similar results were observed in two additional experiments.

Traf3$^{-/-}$ and LMC B cells did not prolong the survival of LMC B cells (Figure S11) and thus exclude the possibility that *Traf3*$^{-/-}$ B cells may constitutively produce prosurvival cytokines (such as BAFF or IL-6). Together, these results indicate that prolonged survival of *Traf3*$^{-/-}$ B cells is due to changes in intrinsic pathways regulating B cell survival or apoptosis.

Increased Nuclear NF-κB2 and Decreased Nuclear PKCδ in *Traf3*$^{-/-}$ B Cells

Activation of both NF-κB1 and NF-κB2 promotes B cell survival, and PKCδ nuclear translocation induces B cell apoptosis (Claudio et al., 2002; Mecklenbrauker et al., 2004; Sasaki et al., 2006). We thus assessed whether TRAF3 deficiency alters these pathways. CD40-induced

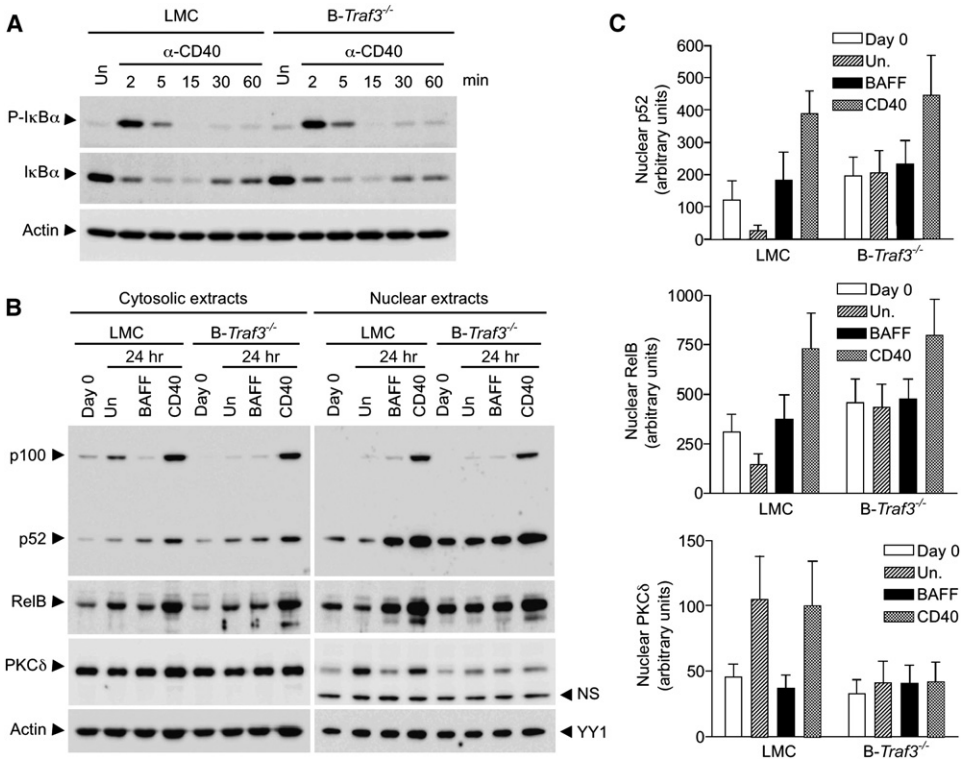

Figure 5. Increased NF-κB2 Activation and Decreased Nuclear PKCδ in *Traf3*$^{-/-}$ B Cells

Resting splenic B cells were purified from 10- to 12- week-old LMC and B-*Traf3*$^{-/-}$ mice and were cultured ex vivo in the absence or presence of 2 μg/ml anti-CD40 for indicated times.

(A) NF-κB1 activation. Total cellular lysates were immunoblotted for phosphorylated (P-) or total IκBα and then immunoblotted for actin.

(B) NF-κB2 activation and PKCδ nuclear translocation. Cytosolic and nuclear extracts were immunoblotted for NF-κB2 (p100-p52), RelB, and PKCδ and then immunoblotted for actin (used as loading control for cytosolic proteins) or YY1 (used as loading control for nuclear proteins).

(C) Quantitation of nuclear p52, RelB, and PKCδ protein amounts. Nuclear p52, RelB and PKCδ bands on immunoblots (right panel of [B]) were quantitated with a low-light imaging system, and the results were presented graphically. The amount of p52, RelB, or PKCδ in each lane was normalized to the intensity of the corresponding YY1 band. The graph depicts the results of three independent experiments (mean ± SEM).

phosphorylation and degradation of IκBα, the hallmark of NF-κB1 activation, was similar in *Traf3*$^{-/-}$ and LMC B cells (Figure 5A). Similarly, CD40-induced phosphorylation of JNK, p38, and ERK was unaltered in *Traf3*$^{-/-}$ B cells (Figure S12). Activation of NF-κB2 requires the processing of the inactive precursor p100 to p52 in the cytosol, and this processing allows the p52-RelB dimer to translocate into the nucleus for activation of transcription of target genes. Ex vivo culture of purified LMC B cells for 24 hr, equivalent to deprivation of endogenous B cell survival factor(s) such as BAFF (Claudio et al., 2002), resulted in an increase in the cytosolic p100 amount and a decrease in nuclear p52 and RelB (Figures 5B and 5C). In contrast, BAFF stimulation decreased the cytosolic p100 but sharply increased nuclear p52 and RelB in LMC B cells. However, such changes in cytosolic p100 or nuclear p52 and RelB amounts induced by deprivation of survival factors or BAFF stimulation were not observed in *Traf3*$^{-/-}$ B cells. These cells did remain responsive to CD40 engagement, which further increased nuclear p52 and RelB amounts similar to those observed in LMC B cells. Interestingly, *Traf3*$^{-/-}$ B cells also displayed lower amounts of nuclear PKCδ compared to LMC B cells, although the amounts of cytosolic PKCδ were comparable (Figures 5B and 5C). Thus, *Traf3*$^{-/-}$ B cells exhibited markedly increased constitutive activation of NF-κB2 and decreased PKCδ nuclear translocation, and both these effects enhance the survival capacity of these cells.

Independence of *Traf3*$^{-/-}$ B Cell Hyperplasia on BAFF or APRIL Signaling

To address whether TRAF3 functions as a downstream negative regulator of BAFF signals for inhibition of peripheral B cell survival, we examined the effects of in vivo administration of TACI-Ig, a soluble fusion protein that blocks both BAFF and APRIL from binding to their receptors (Gross et al., 2001), in B-*Traf3*$^{-/-}$ and LMC mice. Although administration of TACI-Ig effectively reduced the spleen weight and depleted B cells in spleen and LNs of LMC mice, it was unable to reduce the spleen weight or B cell numbers in spleen and LNs of B-*Traf3*$^{-/-}$ mice (Figure 6). Analysis of B cell subsets indicated that TACI-Ig treatment decreased the proportions of mature B (B220^{+}AA4.1^{-}) and especially marginal zone B

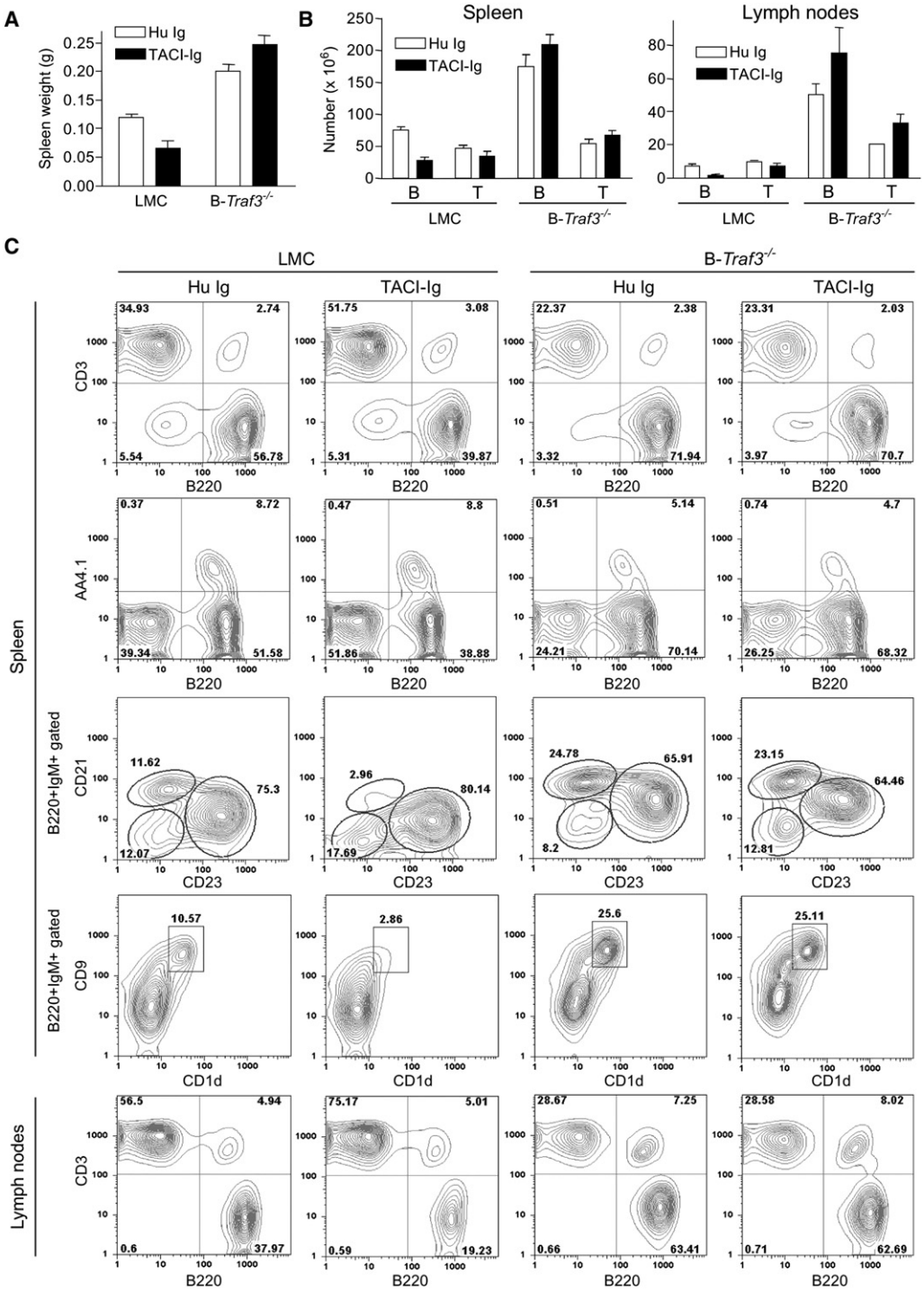

Figure 6. Independence of *Traf3*$^{-/-}$ B Cell Hyperplasia from BAFF and APRIL Signaling

LMC and B-*Traf3*$^{-/-}$ mice (10 weeks old, n = 2 for each group) were i.p. injected with TACI-Ig or a control human Ig Fc (Hu Ig).

(A) Unreduced spleen weight of B-*Traf3*$^{-/-}$ mice after in vivo administration of TACI-Ig. The graph shows the results of two independent experiments (mean ± SE).

(B) Failure of TACI-Ig to decrease the percentages and numbers of B cells in spleen and LNs of B-*Traf3*$^{-/-}$ mice. B and T cells were identified by FACS analysis with B220 and anti-CD3. The graph depicts the results of two independent experiments (mean ± SE).

(C) Representative FACS histograms or contour plots of splenocytes and LN cells after TACI-Ig or Hu Ig administration. FACS profiles were scatter-gated on single lymphocytes. Similar results were observed in a second experiment.

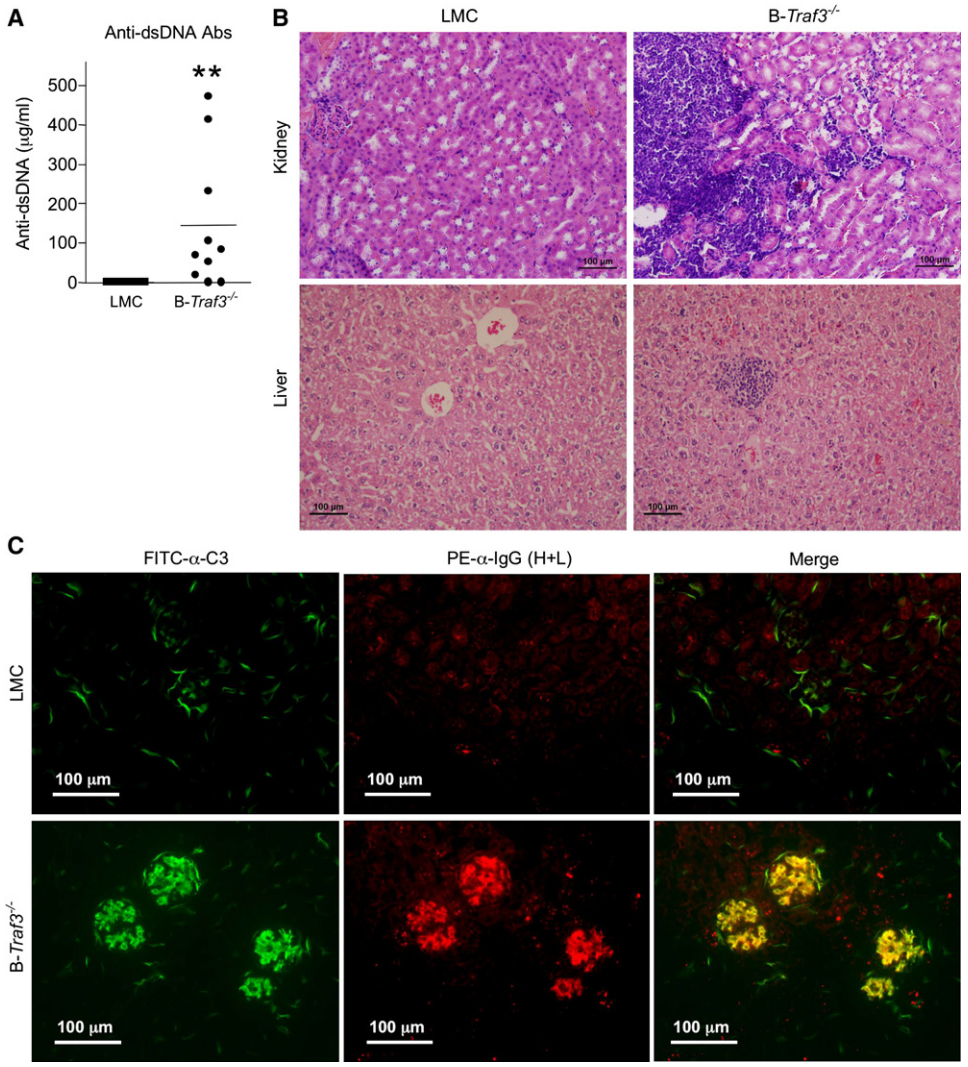

Figure 7. Autoimmune Manifestations in B-*Traf3*$^{-/-}$ Mice

(A) DsDNA autoantibodies in sera of B-*Traf3*$^{-/-}$ mice. Sera from naive LMC and B-*Traf3*$^{-/-}$ mice (n = 10 for each group) were tested for dsDNA autoantibodies by ELISA. Mice analyzed were 10 to 12 weeks old. **, highly significantly different from LMC (t test, $p < 0.001$).

(B) Lymphocyte infiltrations in kidney and liver of B-*Traf3*$^{-/-}$ mice. Microsections of kidneys and livers were stained with hematoxylin and eosin, and representative micrographs of LMC and B-*Traf3*$^{-/-}$ mice are shown for comparison.

(C) Immune-complex deposition in kidney of B-*Traf3*$^{-/-}$ mice. Cryosections of kidneys were blocked and stained with anti-C3-FITC (green, micrographs shown in the left panel) and anti-IgG (H+L)-PE (red, micrographs shown in the middle panel). The right panel shows the merged C3 and IgG (H+L) staining, and yellow color indicates colocalized staining. Mice analyzed in (B) and (C) were 9 to 12 months old, and similar results were observed in two additional experiments.

($B220^+IgM^+CD21^{hi}CD23^{int}$ or $B220^+IgM^+CD1d^+CD9^+$) cells in LMC mice, but not in B-*Traf3*$^{-/-}$ mice (Figure 6C). These data indicate that *Traf3*$^{-/-}$ B cell hyperplasia does not require BAFF or APRIL binding, suggesting that TRAF3 may constitutively inhibit NF-κB2 activation and promote PKCδ nuclear translocation to induce spontaneous apoptosis in peripheral B cells.

Autoimmune Manifestations in B-*Traf3*$^{-/-}$ Mice

In light of the notion that prolonged survival of B cells may contribute to autoimmune diseases (Gauld et al., 2006; Mackay and Kalled, 2002), the spontaneous GC formation in B-*Traf3*$^{-/-}$ mice (Figure 2) prompted us to evaluate whether these mice develop autoimmune diseases. Interestingly, 80% (n = 10) of B-*Traf3*$^{-/-}$ mice already displayed dsDNA autoantibodies in sera at an early age (10–12 weeks), and these autoantibodies were not detected in any LMC mice (n = 10) (Figure 7A and Figure S13). All aged B-*Traf3*$^{-/-}$ mice examined (n = 4, 9 to 12 months old), but none of LMC mice (n = 4), had dsDNA autoantibodies in sera (data not shown). Subsequent histopathological examination revealed that three out of the four

aged B-*Traf3*$^{-/-}$ mice, but none of the LMC mice, contained lymphocyte infiltrates at multiple locations in kidney and liver (Figure 7B and data not shown). Furthermore, these three aged B-*Traf3*$^{-/-}$ mice exhibited immune-complex deposition in kidney as evidenced by the colocalized mesangial staining of IgG (H+L) and complement 3 (C3) at glomeruli. Such colocalized staining was not detected in any of the LMC mice (Figure 7C). Thus, specific ablation of TRAF3 in the B cell lineage can be sufficient for inducing autoimmune manifestations on the B6 X 129 genetic background.

DISCUSSION

To circumvent the limitations posed by the early lethality of *Traf3*$^{-/-}$ mice (Xu et al., 1996), we produced and validated *Traf3*$^{flox/flox}$ mice to allow precise spatial and temporal ablation of TRAF3 expression in the whole animal. This model will be valuable in elucidating the physiological function of TRAF3 in various cell lineages and developmental stages. Our initial characterization of this model revealed a critical role for TRAF3 in inhibiting B cell survival in secondary lymphoid organs and raises the intriguing possibility that TRAF3 is involved in the regulation of self-tolerance.

B-*Traf3*$^{-/-}$ mice exhibited B cell expansion from the T2 transitional stage onward, leading to splenomegaly and lymphadenopathy, hypergammaglobulinemia, and autoimmunity, all of which are remarkably similar to the phenotypes of BAFF-transgenic mice and PKCδ-deficient mice (Gross et al., 2000; Khare et al., 2000; Mackay et al., 1999; Mecklenbrauker et al., 2004; Mecklenbrauker et al., 2002; Miyamoto et al., 2002). Conversely, A/WySnJ mice (carrying a naturally occurring mutation in the BAFF-R gene) and mice deficient in BAFF, BAFF-R, or NF-κB2 display specific B cell loss from the T2 transitional stage onward in peripheral lymphoid organs (Franzoso et al., 1998; Schiemann et al., 2001; Shulga-Morskaya et al., 2004; Thompson et al., 2001). Moreover, *Traf3*$^{-/-}$ B cells showed vastly prolonged survival ex vivo, markedly increased constitutive activation of NF-κB2, and decreased PKCδ nuclear translocation independent of BAFF. These observations led us to test the hypothesis that TRAF3 functions as a downstream negative regulator of BAFF and BAFF-R signaling. However, in vivo administration of TACI-Ig, a potent blocker of BAFF and APRIL signals, failed to deplete peripheral B cells in B-*Traf3*$^{-/-}$ mice. Thus, it is more likely that TRAF3 constitutively inhibits NF-κB2 activation and promotes PKCδ nuclear translocation to induce spontaneous apoptosis in peripheral B cells. In support of this possibility, a previous study provided in vitro evidence that TRAF3 constitutively targets NIK, an upstream kinase required for the activation of NF-κB2, for ubiquitination and proteosome-mediated degradation (Liao et al., 2004). Although we could not reproducibly detect NIK protein in *Traf3*$^{+/+}$ or *Traf3*$^{-/-}$ B cells either in the absence or presence of the proteosome inhibitor MG132 (data not shown), a recent study reported that the amount of NIK protein is increased in *Traf3*$^{-/-}$ B cells and MEFs (He et al., 2006), further suggesting that TRAF3 may constitutively target NIK for degradation to inhibit NF-κB2 activation. How TRAF3 constitutively promotes PKCδ nuclear translocation remains to be determined.

In this study, we extended our findings obtained with *Traf3*$^{-/-}$ B cell lines that CD40-induced NF-κB1, p38, and ERK activation is not affected by TRAF3 deficiency (Xie et al., 2004) to *Traf3*$^{-/-}$ splenic B cells. However, CD40-induced JNK activation is increased in *Traf3*$^{-/-}$ B cell lines (Xie et al., 2004) but appears to be normal in *Traf3*$^{-/-}$ splenic B cells. This difference may be due to the different cellular context of B cell lines versus primary splenic B cells. One possibility is that transformed B cell lines may carry mutations in certain genes, whose altered functions may make CD40-induced JNK activation more sensitive to the loss of TRAF3. Another possibility is that because *Traf3*$^{-/-}$ splenic B cells developed from pro-B, pre-B, and immature B cells in the absence of TRAF3, they may adjust the expression of relevant genes to counteract the deficiency of TRAF3, which might otherwise be detrimental to the development of B cells. Thus, the cell lines may also reflect the effect of TRAF3 deletion only after B cells have completely matured. Both findings may have physiological relevance: Splenic B cells may reflect the situation of altered development in the absence of TRAF3 function, whereas B cell lines may represent the responses in the case of oncogenic transformation, or loss of TRAF3 after complete B cell maturation. In this regard, it should be noted that the expression of TRAF2 is unaltered in *Traf3*$^{-/-}$ B cell lines (Xie et al., 2004) but is increased in *Traf3*$^{-/-}$ splenic B cells (Figure 1A). A similar upregulation of TRAF3 expression was observed in *Traf2*$^{-/-}$ splenic B cells (Grech et al., 2004). Interestingly, conditional *Traf2*$^{-/-}$ mice also display expanded B cell compartments in spleen and LNs, and *Traf2*$^{-/-}$ B cells also show increased constitutive NF-κB2 activation ex vivo (Grech et al., 2004). Thus, TRAF2 and TRAF3 may have redundant function in inhibiting constitutive NF-κB2 activation and B cell survival, and upregulation of either of these TRAF molecules may partially compensate for the loss of the other.

The B cell is the central player in humoral immunity. Interestingly, we observed that basal serum titers of various Ig isotypes were generally elevated in B-*Traf3*$^{-/-}$ mice, with the exception of IgG1 and IgE. Similarly, antibody responses, including IgM and all IgG isotypes, to a T-I Ag were increased in B-*Traf3*$^{-/-}$ mice. Because antibody responses to TNP-Ficoll are mainly mediated by MZ B cells (Pillai et al., 2005), the increased Ig responses to TNP-Ficoll immunization are consistent with the vastly expanded MZ B cells in these mice. However, in response to the T-D Ag TNP-KLH, although TNP-specific IgM was increased, IgG1 was not increased accordingly. Considering that mature B cells, including follicular and MZ B cells, were markedly expanded in B-*Traf3*$^{-/-}$ mice, it is perplexing that these mice displayed neither an increase in the T-D IgG1 response nor an elevation in basal serum IgG1 or IgE titers. It is known that isotype switching to both IgG1 and IgE is regulated by CD40 and IL-4 (Stavnezer and Amemiya, 2004). One

possibility is that TRAF3 may participate in this process. Because IgG1 is the major antibody produced in T dependent responses to bacterial pathogens and soluble protein antigens in mice (Stavnezer and Amemiya, 2004), lack of increase of basal serum IgG1 titer may partially reflect the lack of increase in T dependent IgG1 responses in B-*Traf3*$^{-/-}$ mice. Notably, previous studies indicate that CD21 and CD23 play a modulatory role in antibody responses (Haas et al., 2002; Texido et al., 1994; Yu et al., 1994). Thus, it is also possible that the enhanced expression of CD21 and CD23 on B cells may contribute to the serological phenotype of B-*Traf3*$^{-/-}$ mice.

Increasing evidence suggests that prolonged survival of B cells contributes to autoimmune diseases (Gauld et al., 2006; Mackay and Kalled, 2002). Peripheral self-tolerance is induced through anergy, defined as functional inactivation of autoreactive B cells (Gauld et al., 2006). Prolonged survival of anergic B cells can lead to autoimmunity, simply by providing a greater opportunity for anergic B cells to be recruited to an immune response (Gauld et al., 2006; Mackay and Kalled, 2002). Interestingly, anergic B cells have increased dependence on BAFF for survival and cannot compete with normal B cells for a limiting source of BAFF (Gauld et al., 2006; Lesley et al., 2004). Thus, the prolonged BAFF-independent survival capacity of *Traf3*$^{-/-}$ B cells may predispose B-*Traf3*$^{-/-}$ mice to develop autoimmune reactivity. Indeed, the majority of B-*Traf3*$^{-/-}$ mice already exhibited numerous and large spontaneous splenic GCs in the absence of immunization and developed dsDNA autoantibodies in the serum by the age of 10–12 weeks. Furthermore, aged B-*Traf3*$^{-/-}$ mice developed additional autoimmune manifestations, including lymphocyte infiltration in kidney and liver, and immune-complex deposition in kidney. Thus, specific deletion of TRAF3 in B cells appears to be sufficient for inducing autoimmune alterations in mice. However, it should be noted that B-*Traf3*$^{-/-}$ mice had a mixed genetic background of B6 X 129 and that epistatic interactions between the B6 and 129 genomes have important impacts on systemic autoimmune manifestations (Manderson et al., 2004; McDonnell et al., 1989; Strasser et al., 1991; Wakeland et al., 2001). Thus, the mixed genetic background of B6 X 129 may make the mice more sensitive to the loss of TRAF3 and prone to autoimmune alterations. Nevertheless, our results indicate that TRAF3 deficiency can be a predisposing genetic factor to autoimmune diseases in mice.

Extended lifespan of B cells and B cell hyperplasia have been associated with B leukemiagenesis and B lymphomagenesis (Cory et al., 2003; Mackay and Tangye, 2004; Packham and Stevenson, 2005). Whether B-*Traf3*$^{-/-}$ mice have increased propensity to develop lymphomas awaits investigation. Nonetheless, prolonged survival of *Traf3*$^{-/-}$ B cells could predispose them to transformation in response to additional oncogenic events, such as viral infections, chronic inflammation, mutations, or chromosomal translocations involving oncogenes or tumor suppressor genes. Consistent with this, elevated serum BAFF has been detected in humans with autoimmune diseases as well as B cell malignancies (Mackay and Tangye, 2004). Caused by chromosomal translocations, constitutively activated mutant forms of NF-κB2 have also been detected in patients with B lymphomas (Karin et al., 2002). It would thus be interesting to investigate whether inactivating mutations of the *Traf3* gene or decreased expression of TRAF3 occur in human patients with autoimmune diseases as well as B leukemias or lymphomas. The new mouse model presented here suggests that specifically enhancing TRAF3 activity or expression in B cells may be of therapeutic value in combating these human diseases.

EXPERIMENTAL PROCEDURES

Generation of Conditional *Traf3*$^{-/-}$ Mice

Traf3$^{+/flox}$ mice were generated in accordance with standard protocols as detailed in the Supplemental Experimental Procedures and were interbred for generation of *Traf3*$^{flox/flox}$ mice. *Traf3*$^{flox/flox}$ mice were crossed with *Cd19*$^{Cre/Cre}$ mice (Rickert et al., 1997) (Jackson Laboratory) for generation of *Traf3*$^{+/flox}$*Cd19*$^{+/Cre}$ mice, which were subsequently backcrossed with *Traf3*$^{flox/flox}$ mice for generation of *Traf3*$^{flox/flox}$*Cd19*$^{+/Cre}$ (B-*Traf3*$^{-/-}$) mice. Deletion of exons 1 and 2 of the *Traf3* gene in splenic B cells was detected by genomic PCR with primers U7 and BT6 (Figure S1C). B-*Traf3*$^{-/-}$ mice that were analyzed had a mixed genetic background between 129/SvJ and C57BL/6, and littermates were used as controls for all experiments. All mice were kept in specific pathogen-free conditions in the Gene Targeting Core Facility at the University of Iowa and were used in accordance with NIH guidelines and under an animal protocol approved by the Animal Care and Use Committee of the University of Iowa.

Primers, Antibodies, Reagents, and Methods for Supplemental Figures

Details of primers, Abs, reagents, and methods for supplemental figures are described in the Supplemental Experimental Procedures.

Flow Cytometry

Single-cell suspensions were made from the spleen, LNs, thymus, BM, and peritoneal lavages. Erythrocytes from spleen were depleted with ACK lysis buffer. Cells (0.5×10^6) were then blocked with rat serum and FcR blocking Ab (2.4G2) and incubated with various Abs conjugated to FITC, PE, PerCP, or Cy5 for multiple color fluorescence surface staining. For cellularity analysis, cell-surface markers examined include CD45R (B220), CD3, AA4.1, c-Kit, CD25, CD1d, CD9, CD19, CD21, CD23, CD5, IgM, IgD, CD38, CD43, CD4, CD8, CD11b, Gr-1, and MHC class II (I-A/I-E) as indicated in the figures and Table S1. List-mode data were acquired on a FACSVantage (Becton Dickinson) with Cell Quest software. The results were analyzed with FlowJo software (TreeStar). FSC-SSC gating for single lymphocytes, excluding cell aggregates, small erythrocytes, and dead cell debris, was used for analyzing flow-cytometric data.

Hematoxylin-Eosin Staining of Tissues

Mouse LNs, kidney, and liver were fixed in 10% neutral formalin, then processed and embedded in paraffin. Microsections (5 μm) of paraffin blocks were prepared with a microtome (HM 355, Microm) and were stained with hematoxylin and eosin with an automated slide stainer (Sakura DRS 601 Diversified Stainer, Sakura). Stained slides were mounted with Solvent 100 mounting media, and bright-field micrographs of stained sections were taken with a microscope (Olympus BX-51, Olympus America) fitted with an Olympus DP70 camera (Olympus America).

Immunohistochemistry

Spleens were harvested from naive mice or mice immunized i.p. with 0.1 ml of 10% SRBC in PBS for 10 days. Kidneys were collected

from aged naive mice. Tissues were soaked in 20% sucrose in PBS for 20 min, embedded with OCT compound, and snap frozen in liquid N2. Frozen sections (8–10 μm) were prepared with a cryostat (HM505E, Microm) and fixed with cold acetone. Rehydration, blocking, and staining of sections were carried out as described (Stunz et al., 2004). Spleen sections were stained with FITC-PNA, Alexa Fluor 350-anti-mouse IgM Ab, and PE-anti-mouse CD3 Ab so that splenic architecture could be determined, or sections were stained with FITC-anti-mouse MOMA-1 Ab and PE-B220 for visualization of MZ B cells. Kidney sections were stained with FITC-anti-mouse C3 Ab and PE-anti-mouse IgG (H+L) Ab. Stained slides were mounted with Vector-Shield and observed on a fluorescence microscope (Olympus BX-60, Olympus America) fitted with a Sensys camera (Photometrics). Images were analyzed with ImagePro4.5 software (Media Cybernetics).

Immunizations and ELISAs

Basal-serum titers of various Ig isotypes were analyzed by ELISA as previously described (Stunz et al., 2004). In the IgE-specific ELISA, capture mAb was EM95, and detection Ab was Alkaline phosphatase (AP)-conjugated goat anti-mouse IgE Ab. All the other capture Abs and AP-conjugated detection Abs were polyclonal goat Abs, including Abs specific for mouse IgM, IgG1, IgG2a, IgG2b, IgG3, and IgA. Plates were read on a Versamax plate reader (Molecular Devices), and results were analyzed with SoftMax Pro 4.0 software. Standard curves were included on each plate in accordance with purified standards (Southern Biotechnology Associates) for each Ig isotype.

For T-I antibody responses, mice were immunized i.p. with 50 μg of TNP-Ficoll (Biosource Technologies) precipitated in alum. Sera were collected on day 10 after immunization. TNP-specific Abs in sera were measured with the use of ELISA plates coated with TNP_{38}-conjugated bovine-serum albumin. Bound Abs were detected with AP-conjugated goat anti-mouse IgM, IgG1, IgG2a, IgG2b, or IgG3, respectively. For T-D antibody responses, mice were immunized i.p. with 100 μg of TNP-KLH (Biosource Technologies) precipitated in alum and boosted with 100 μg of TNP-KLH in alum on day 21. Sera were collected on day 7, 14, and 28 after the first immunization. Serum titers of anti-TNP IgM and IgG1 were measured by ELISA as described above. For TNP-specific IgG1 or IgG2a, standard curves were determined on each plate with serial dilutions of purified standards (BD PharMingen). For TNP-specific IgM, IgG2b, or IgG3, standard curves were determined on each plate with serial dilutions of a standard serum. Multiple 1:5 or 1:10 serial dilutions of each serum sample were examined in each TNP-specific Ig isotype ELISA, and the range of the dilution factors tested is from 1:100 to 1:1000000. Each standard curve contained 11 dilution points, and in all cases, the coefficient of determination for the standard curve (r^2) was >0.98. The dilution factor that gave A405 (O.D.405 nm) values within the linear range (0.1∼1.5) of standard curves of ELISA was used for calculating the concentrations of TNP-specific IgG1 and IgG2a or the relative titers of TNP-specific IgM, IgG2b, and IgG3. Relative titers were calculated according to the formula "relative titer = A405 value × 10 × dilution factor," and therefore reflect the relative concentrations of each TNP-specific Ig isotype in arbitrary units.

Splenic B Cell Purification

Splenic B cells and non-B cells were separated with anti-mouse CD43-coated magnetic beads and a MACS separator (Miltenyi Biotec) in accordance with the manufacturer's protocols. For purification of resting splenic B cells, high-density resting splenocytes were first isolated by density gradient centrifugation through a 60%:65%:85% Percoll gradient. Resting lymphocytes at the interface between 65% and 85% Percoll were collected, and resting B cells were further purified by negative selection with anti-mouse CD43 magnetic beads according to the manufacturer's protocols. The purity of isolated populations was monitored by FACS analysis with Cy5-anti-B220, FITC-anti-IgM and PE-anti-Fas, and cell preparations of >90% purity were used for further experiments. Purified resting splenic B cells were cultured in mouse-culture medium (RPMI 1640 medium supplemented with 5% FCS, 10 μM β-mercaptoethanol, 10 mM HEPES [pH 7.55], 1 mM sodium pyruvate, 2 mM L-glutamine, and 0.1 mM nonessential amino acids).

Survival Assay and Cell-Cycle Analysis

Purified resting splenic B cells (0.5 × 10^6/ml/well) were cultured in 24-well plates in the absence or presence of 0.5 μg/ml BAFF or 2 μg/ml of anti-mouse CD40 Ab (HM40-3) at 37°C. Cells were fed with fresh medium containing the appropriate stimulation every 4 days. At each time point, the number of viable cells was determined by staining with Trypan blue. For PI staining, cells were fixed with an equal volume of ice-cold 70% ethanol. PI staining was performed as previously described (Catlett et al., 2001), and DNA content was quantified with a benchtop FACScan (Becton Dickinson). Labeling of B cells with CFSE (Molecular Probes) for proliferation analysis was performed in accordance with the manufacturer's instructions. Labeled cells were cultured in the absence or presence of 2 μg/ml of anti-mouse CD40 (HM40-3) alone or in combination with 10 μg/ml of anti-mouse IgM (Fab') or 100 ng/ml of IL-4 at 37°C for 4 days. Cells were then fixed, and the decline in CFSE fluorescence as a measure of proliferation was determined by FACS analysis.

Immunoblot Analysis

For detection of TRAF3 expression in B cells versus non-B cells, purified $CD43^+$ and $CD43^-$ splenocytes were directly lysed as previously described (Xie and Bishop, 2004). For detection of the activation of NF-κB1 or MAP kinases, purified resting splenic B cells were cultured in the absence or presence of 2 μg/ml of anti-mouse CD40 (HM40-3) at 37°C for various time periods as indicated in the figures, and total cellular lysates were prepared. For detection of nuclear translocation of NF-κB2 and PKCδ, purified resting splenic B cells were cultured in the absence or presence of 0.5 μg/ml BAFF or 2 μg/ml of anti-mouse CD40 (HM40-3) at 37°C for 24 hr. Cytosolic and nuclear extracts were prepared as described (Xie et al., 2006). Immunoblot analysis was performed with various antibodies as previously described (Xie and Bishop, 2004). Protein bands on immunoblots were quantitated with a low-light imaging system (LAS-1000, FUJIFILM Medical Systems USA).

In Vivo Administration of TACI-Ig

Mice (10 weeks old) were injected i.p. with 100 μg of TACI-Ig (R&D Systems) or a control Ig (human Ig Fc) three times a week for 15 days.

Detection of dsDNA Autoantibodies

Sera from naive mice were tested for autoantibodies with ELISA kits detecting dsDNA Abs (Alpha Diagnostic) in accordance with the manufacturer's protocols. Standards and negative and positive control sera provided by the manufacturer were run concurrently with the unknown samples. The specificity of dsDNA autoantibodies detected in B-*Traf3*$^{-/-}$ mice was verified by a second assay with *Crithidia luciliae* dsDNA substrate slides (The Binding Site) as previously described (Stunz et al., 2004).

Statistics

For direct comparison of spontaneous GC B cells and Ig isotype titers of LMC and B-*Traf3*$^{-/-}$ mice, statistical significance was determined with the unpaired t test for two-tailed data. All p values less than 0.05 are considered significant, and p values less than 0.01 are considered very significant.

Supplemental Data

Additional Experimental Procedures, 14 figures, and one table are available at http://www.immunity.com/cgi/content/full/27/2/253/DC1/.

ACKNOWLEDGMENTS

This study was supported by a National Scientist Development grant from the American Heart Association (P. Xie), and National Institutes

of Health grants AI28847, AI49993, CA099997, and a VA Career Award (G. Bishop). We are grateful to T. Waldschmidt for his expert advice on FACS data analysis, and D. Meyerholz for pathological evaluation of HE- and immunofluorescence- stained tissue sections. We would like to thank T. Kinney for expert animal husbandry, K. Oxley for excellent technical assistance, K. Walters and C. Allamargot of the Central Microscopy Research Facility for technical help in microsection and HE staining, and J. Houtman and B. Hostager for stimulating discussions and critical review of the manuscript.

Received: October 4, 2006
Revised: April 27, 2007
Accepted: July 6, 2007
Published online: August 23, 2007

REFERENCES

Bishop, G.A. (2004). The multifaceted roles of TRAFs in the regulation of B-cell function. Nat. Rev. Immunol. *4*, 775–786.

Catlett, I.M., Xie, P., Hostager, B.S., and Bishop, G.A. (2001). Signaling through MHC class II molecules blocks CD95-induced apoptosis. J. Immunol. *166*, 6019–6024.

Claudio, E., Brown, K., Park, S., Wang, H., and Siebenlist, U. (2002). BAFF-induced NEMO-independent processing of NF-kappa B2 in maturing B cells. Nat. Immunol. *3*, 958–965.

Cory, S., Huang, D.C., and Adams, J.M. (2003). The Bcl-2 family: Roles in cell survival and oncogenesis. Oncogene *22*, 8590–8607.

Franzoso, G., Carlson, L., Poljak, L., Shores, E.W., Epstein, S., Leonardi, A., Grinberg, A., Tran, T., Scharton-Kersten, T., Anver, M., et al. (1998). Mice deficient in nuclear factor (NF)-kappa B/p52 present with defects in humoral responses, germinal center reactions, and splenic microarchitecture. J. Exp. Med. *187*, 147–159.

Gauld, S.B., Merrell, K.T., and Cambier, J.C. (2006). Silencing of autoreactive B cells by anergy: A fresh perspective. Curr. Opin. Immunol. *18*, 292–297.

Grammer, A.C., and Lipsky, P.E. (2000). CD40-mediated regulation of immune responses by TRAF-dependent and TRAF-independent signaling mechanisms. Adv. Immunol. *76*, 61–178.

Grech, A.P., Amesbury, M., Chan, T., Gardam, S., Basten, A., and Brink, R. (2004). TRAF2 differentially regulates the canonical and noncanonical pathways of NF-kappaB activation in mature B cells. Immunity *21*, 629–642.

Gross, J.A., Dillon, S.R., Mudri, S., Johnston, J., Littau, A., Roque, R., Rixon, M., Schou, O., Foley, K.P., Haugen, H., et al. (2001). TACI-Ig neutralizes molecules critical for B cell development and autoimmune disease. impaired B cell maturation in mice lacking BLyS. Immunity *15*, 289–302.

Gross, J.A., Johnston, J., Mudri, S., Enselman, R., Dillon, S.R., Madden, K., Xu, W., Parrish-Novak, J., Foster, D., Lofton-Day, C., et al. (2000). TACI and BCMA are receptors for a TNF homologue implicated in B-cell autoimmune disease. Nature *404*, 995–999.

Haas, K.M., Hasegawa, M., Steeber, D.A., Poe, J.C., Zabel, M.D., Bock, C.B., Karp, D.R., Briles, D.E., Weis, J.H., and Tedder, T.F. (2002). Complement receptors CD21/35 link innate and protective immunity during Streptococcus pneumoniae infection by regulating IgG3 antibody responses. Immunity *17*, 713–723.

Hacker, H., Redecke, V., Blagoev, B., Kratchmarova, I., Hsu, L.C., Wang, G.G., Kamps, M.P., Raz, E., Wagner, H., Hacker, G., et al. (2006). Specificity in Toll-like receptor signalling through distinct effector functions of TRAF3 and TRAF6. Nature *439*, 204–207.

He, J.Q., Zarnegar, B., Oganesyan, G., Saha, S.K., Yamazaki, S., Doyle, S.E., Dempsey, P.W., and Cheng, G. (2006). Rescue of TRAF3-null mice by p100 NF-kappa B deficiency. J. Exp. Med. *203*, 2413–2418.

Karin, M., Cao, Y., Greten, F.R., and Li, Z.W. (2002). NF-kappaB in cancer: From innocent bystander to major culprit. Nat. Rev. Cancer *2*, 301–310.

Khare, S.D., Sarosi, I., Xia, X.Z., McCabe, S., Miner, K., Solovyev, I., Hawkins, N., Kelley, M., Chang, D., Van, G., et al. (2000). Severe B cell hyperplasia and autoimmune disease in TALL-1 transgenic mice. Proc. Natl. Acad. Sci. USA *97*, 3370–3375.

Lesley, R., Xu, Y., Kalled, S.L., Hess, D.M., Schwab, S.R., Shu, H.B., and Cyster, J.G. (2004). Reduced competitiveness of autoantigen-engaged B cells due to increased dependence on BAFF. Immunity *20*, 441–453.

Liao, G., Zhang, M., Harhaj, E.W., and Sun, S.C. (2004). Regulation of the NF-kappaB-inducing kinase by tumor necrosis factor receptor-associated factor 3-induced degradation. J. Biol. Chem. *279*, 26243–26250.

Mackay, F., and Kalled, S.L. (2002). TNF ligands and receptors in autoimmunity: An update. Curr. Opin. Immunol. *14*, 783–790.

Mackay, F., Schneider, P., Rennert, P., and Browning, J. (2003). BAFF AND APRIL: A tutorial on B cell survival. Annu. Rev. Immunol. *21*, 231–264.

Mackay, F., and Tangye, S.G. (2004). The role of the BAFF/APRIL system in B cell homeostasis and lymphoid cancers. Curr. Opin. Pharmacol. *4*, 347–354.

Mackay, F., Woodcock, S.A., Lawton, P., Ambrose, C., Baetscher, M., Schneider, P., Tschopp, J., and Browning, J.L. (1999). Mice transgenic for BAFF develop lymphocytic disorders along with autoimmune manifestations. J. Exp. Med. *190*, 1697–1710.

Manderson, A.P., Botto, M., and Walport, M.J. (2004). The role of complement in the development of systemic lupus erythematosus. Annu. Rev. Immunol. *22*, 431–456.

McDonnell, T.J., Deane, N., Platt, F.M., Nunez, G., Jaeger, U., McKearn, J.P., and Korsmeyer, S.J. (1989). bcl-2-immunoglobulin transgenic mice demonstrate extended B cell survival and follicular lymphoproliferation. Cell *57*, 79–88.

Mecklenbrauker, I., Kalled, S.L., Leitges, M., Mackay, F., and Tarakhovsky, A. (2004). Regulation of B-cell survival by BAFF-dependent PKCdelta-mediated nuclear signalling. Nature *431*, 456–461.

Mecklenbrauker, I., Saijo, K., Zheng, N.Y., Leitges, M., and Tarakhovsky, A. (2002). Protein kinase Cdelta controls self-antigen-induced B-cell tolerance. Nature *416*, 860–865.

Miller, J.P., Stadanlick, J.E., and Cancro, M.P. (2006). Space, selection, and surveillance: Setting boundaries with BLyS. J. Immunol. *176*, 6405–6410.

Miyamoto, A., Nakayama, K., Imaki, H., Hirose, S., Jiang, Y., Abe, M., Tsukiyama, T., Nagahama, H., Ohno, S., Hatakeyama, S., and Nakayama, K.I. (2002). Increased proliferation of B cells and autoimmunity in mice lacking protein kinase Cdelta. Nature *416*, 865–869.

Morrison, M.D., Reiley, W., Zhang, M., and Sun, S.C. (2005). An atypical tumor necrosis factor (TNF) receptor-associated factor-binding motif of B cell-activating factor belonging to the TNF family (BAFF) receptor mediates induction of the noncanonical NF-kappaB signaling pathway. J. Biol. Chem. *280*, 10018–10024.

Oganesyan, G., Saha, S.K., Guo, B., He, J.Q., Shahangian, A., Zarnegar, B., Perry, A., and Cheng, G. (2006). Critical role of TRAF3 in the Toll-like receptor-dependent and -independent antiviral response. Nature *439*, 208–211.

Packham, G., and Stevenson, F.K. (2005). Bodyguards and assassins: Bcl-2 family proteins and apoptosis control in chronic lymphocytic leukaemia. Immunology *114*, 441–449.

Pasparakis, M., Schmidt-Supprian, M., and Rajewsky, K. (2002). IkappaB kinase signaling is essential for maintenance of mature B cells. J. Exp. Med. *196*, 743–752.

Pillai, S., Cariappa, A., and Moran, S.T. (2005). Marginal zone B cells. Annu. Rev. Immunol. *23*, 161–196.

Quezada, S.A., Jarvinen, L.Z., Lind, E.F., and Noelle, R.J. (2004). CD40/CD154 interactions at the interface of tolerance and immunity. Annu. Rev. Immunol. *22*, 307–328.

Rickert, R.C., Roes, J., and Rajewsky, K. (1997). B lymphocyte-specific, Cre-mediated mutagenesis in mice. Nucleic Acids Res. *25*, 1317–1318.

Sasaki, Y., Derudder, E., Hobeika, E., Pelanda, R., Reth, M., Rajewsky, K., and Schmidt-Supprian, M. (2006). Canonical NF-kappaB activity, dispensable for B cell development, replaces BAFF-receptor signals and promotes B cell proliferation upon activation. Immunity *24*, 729–739.

Schiemann, B., Gommerman, J.L., Vora, K., Cachero, T.G., Shulga-Morskaya, S., Dobles, M., Frew, E., and Scott, M.L. (2001). An essential role for BAFF in the normal development of B cells through a BCMA-independent pathway. Science *293*, 2111–2114.

Shulga-Morskaya, S., Dobles, M., Walsh, M.E., Ng, L.G., MacKay, F., Rao, S.P., Kalled, S.L., and Scott, M.L. (2004). B cell-activating factor belonging to the TNF family acts through separate receptors to support B cell survival and T cell-independent antibody formation. J. Immunol. *173*, 2331–2341.

Stavnezer, J., and Amemiya, C.T. (2004). Evolution of isotype switching. Semin. Immunol. *16*, 257–275.

Strasser, A., Whittingham, S., Vaux, D.L., Bath, M.L., Adams, J.M., Cory, S., and Harris, A.W. (1991). Enforced BCL2 expression in B-lymphoid cells prolongs antibody responses and elicits autoimmune disease. Proc. Natl. Acad. Sci. USA *88*, 8661–8665.

Stunz, L.L., Busch, L.K., Munroe, M.E., Sigmund, C.D., Tygrett, L.T., Waldschmidt, T.J., and Bishop, G.A. (2004). Expression of the cytoplasmic tail of LMP1 in mice induces hyperactivation of B lymphocytes and disordered lymphoid architecture. Immunity *21*, 255–266.

Texido, G., Eibel, H., Le Gros, G., and van der Putten, H. (1994). Transgene CD23 expression on lymphoid cells modulates IgE and IgG1 responses. J. Immunol. *153*, 3028–3042.

Thompson, J.S., Bixler, S.A., Qian, F., Vora, K., Scott, M.L., Cachero, T.G., Hession, C., Schneider, P., Sizing, I.D., Mullen, C., et al. (2001). BAFF-R, a newly identified TNF receptor that specifically interacts with BAFF. Science *293*, 2108–2111.

Wajant, H., Henkler, F., and Scheurich, P. (2001). The TNF-receptor-associated factor family. Scaffold molecules for cytokine receptors, kinases and their regulators. Cell. Signal. *13*, 389–400.

Wakeland, E.K., Liu, K., Graham, R.R., and Behrens, T.W. (2001). Delineating the genetic basis of systemic lupus erythematosus. Immunity *15*, 397–408.

Xie, P., and Bishop, G.A. (2004). Roles of TNF receptor-associated factor 3 in signaling to B lymphocytes by carboxyl-terminal activating regions 1 and 2 of the EBV-encoded oncoprotein latent membrane protein 1. J. Immunol. *173*, 5546–5555.

Xie, P., Hostager, B.S., and Bishop, G.A. (2004). Requirement for TRAF3 in signaling by LMP1 but not CD40 in B lymphocytes. J. Exp. Med. *199*, 661–671.

Xie, P., Hostager, B.S., Munroe, M.E., Moore, C.R., and Bishop, G.A. (2006). Cooperation between TNF receptor-associated factors 1 and 2 in CD40 signaling. J. Immunol. *176*, 5388–5400.

Xu, Y., Cheng, G., and Baltimore, D. (1996). Targeted disruption of TRAF3 leads to postnatal lethality and defective T-dependent immune responses. Immunity *5*, 407–415.

Yu, P., Kosco-Vilbois, M., Richards, M., Kohler, G., and Lamers, M.C. (1994). Negative feedback regulation of IgE synthesis by murine CD23. Nature *369*, 753–756.